Synchronization and multimode dynamics of mutually coupled semiconductor lasers

Claudio R. Mirasso,[1,2] Miroslav Kolesik,[1,3] Marcelo Matus,[1] J. K. White,[4] and Jerome V. Moloney[1]
[1]*Arizona Center for Mathematical Science, University of Arizona, Tucson, Arizona 85721*
[2]*Departament de Física, Universitat de les Illes Balears, E-07071 Palma de Mallorca, Spain*
[3]*Institute of Physics, Slovak Academy of Sciences, Bratislava, Slovakia*
[4]*Nortel Networks, High Performance Optical Component Solutions, 3500 Carling Avenue, Ottawa, Ontario, Canada ON K2H 8E9*
(Received 19 April 2001; published 5 December 2001)

The dynamics of coupled semiconductor lasers is investigated by numerical simulations. A realistic laser simulation engine is used to study the synchronization and dynamical regime in two mutually coupled Fabry-Pérot and/or distributed feedback lasers. Both single- and multimode operation regimes are studied, with emphasis on the role of the multiple laser-cavity modes. Our findings indicate that the two lasers synchronize within each laser-cavity mode, while the synchronization across different cavity modes is significantly weaker.

DOI: 10.1103/PhysRevA.65.013805 PACS number(s): 42.65.Sf, 42.55.Px, 05.45.Xt

Synchronization between coupled nonlinear oscillators has recently attracted the attention of many researchers. A rich palette of behaviors has been observed in a wide variety of systems including, among others, population dynamics, coupled neurons, and lasers [1–5]. The interest in the synchronization between chaotic semiconductor lasers has been motivated by its potential for practical applications, for example, in communication systems using chaos to camouflage the transmitted messages [6,7]. In most cases the coupling between the subsystems includes a delay that accounts for the time the information takes to travel from one subsystem to the other. This delay introduces additional degrees of freedom to the system and leads to a qualitative different dynamics. The effect of the delay between two mutually coupled semiconductor lasers has been studied recently [4,8] in the regime of long delays and moderate injection couplings. A spontaneous symmetry breaking was observed, together with a retarded synchronization of chaotic regimes between the two subsystems. Similar studies, but with weak couplings and short delay times, have demonstrated localized synchronization of relaxation oscillations [12].

A semiconductor laser model, described by partial differential equations and including parabolic gain, was used in Ref. [5] to study feedback effects. In that paper, it was shown that weak external feedback can promote multilongitudinal mode instabilities in an otherwise nominally single-mode semiconductor laser, a fact that was also observed experimentally [9]. Moreover, in Ref. [5] it was found that when two identical semiconductor lasers subjected to optical feedback are coupled unidirectionally, the same individual laser-cavity mode could synchronize to its counterpart even though the other modes might be out of synchronization. Despite the relevance that multimode behavior may have in some cases, the majority of numerical simulations have been carried out with a rate-equation model that assumes a single laser-cavity mode operation and neglects spatial dependencies. Although the agreement between the rate-equation-based models and experimental observations is very good in general, questions concerning the role of multimode laser operation arise [9]. It is possible to extend the Lang-Kobayashi-type models to multimode systems [10], but we feel that the underlying approximations are difficult to control and prefer a more direct approach. The present work aims at further understanding of the multimode behavior in mutually coupled lasers by numerical simulations that are free of the usual rate-equation model approximations. To this end, we use a laser simulator with full spatial and temporal resolution [11]. The simulation engine allows us to perform realistic numerical experiments on systems consisting of various types of semiconductor laser as well as passive cavities and the coupling between the subsystems.

We consider two identical devices, which will be pairs of either Fabry-Pérot (FP) or distributed feedback (DFB) lasers. We pump both lasers with the same injection current very close to their solitary threshold. The distance between the two lasers is set to 1.2 m, or equivalently a flight time for light of $\tau \sim 4$ ns. A neutral density filter reduces the coupling between the lasers, which we fix to a value of 6% of transmission. For the FP laser we consider devices of 250 μm length and 4 μm width with natural, as-cleaved, facet reflectivities. In the case of DFB lasers, we use slightly longer devices (400 μm) with simple Bragg gratings, i.e. without grating phase inserts, with a coupling coefficient of 5000 m^{-1} and zero reflectivity at the facets. Although such devices exhibit two symmetric grating supported modes, due to the asymmetry induced by the coupling with the counterpart laser, the carrier density profiles become asymmetric. This in turn provides slightly different gain for the two grating modes and one of these modes is greatly suppressed. We choose the parameters of both types of laser such that they operate with carrier densities at which the active layer exhibits an α factor around 3.

The simulational model includes full many-body microscopic gain and refractive index and correctly accounts for gain dispersion in a broad frequency band. White noise sources of zero mean and δ correlation in space and time are included in the field equations. The flexibility of the simulator allows us to consider both the FP type and the DFB type of lasers without any restrictions on their modal properties. The simulator also accounts for both mutual injection and feedback coming from the front facet of the counterpart laser. Moreover, the simulator also allows us to check situations in which the optical feedback has negligible effects, as reported in [4,12], but we can anticipate that the results do not change

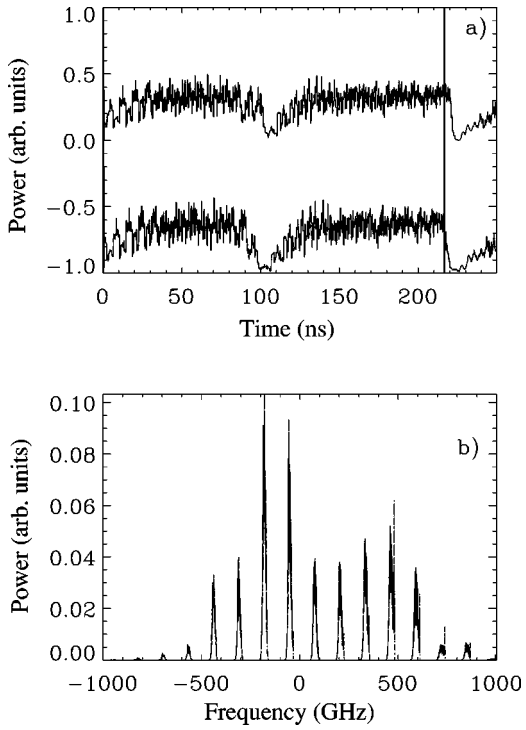

FIG. 1. Output intensity (with a detection bandwidth of 0.5 GHz) of the two coupled Fabry-Pérot lasers (a), and their time-averaged optical spectra (b).

qualitatively. Under these conditions we approach as much as possible the situation reported in recent experiments [4,12].

The main features we observe in the simulations with the FP laser twins can be summarized as follows.

(1) We observe a low frequency fluctuations (LFF) behavior, characterized by a sudden drop of the total intensity, similar to the one reported in Refs. [4,8]. This behavior resembles the well known LFF regime that appears in the case of a laser subjected to optical feedback (see, for example, [13] and references therein). However, we have observed that this regime persists even when we exclude feedback effects from the facet of the other laser, which is an indication that mutual injection alone may induce this kind of instability.

(2) We observe a well defined leader-laggard dynamics, as reported experimentally and numerically with a rate-equation model [4,8], where the role of the leader and laggard changes randomly from one dropout to the next.

(3) We observe a high degree of synchronization between the total output power of both lasers when one of the outputs is shifted with respect to the other by a time τ, τ being the time it takes the light to fly from one laser to the other.

(4) We observe a significant degree of synchronization only if one of the series is shifted with respect to the other by an integer, but odd, multiple of τ.

In Fig. 1 we show the typical time traces of the total output power and the optical spectra of both lasers, the latter being averaged over a whole LFF cycle. In panel (a) the output power of both lasers exhibits the LFF features that we have already mentioned. As expected, fast irregular pulsations, in the gigahertz range, develop within these slow LFF cycles. In panel (b) it can be seen that the lasers operate in a multimode regime. Despite this complicated dynamics, the spectra of the two lasers are so similar to each other that it is very difficult to distinguish them. This is an indication of synchronization between the two lasers. However, these spectra do not tell us much about the dynamical evolution of the individual longitudinal modes. To gain insight into this problem we concentrate on the dynamics that take place within the different longitudinal modes of the FP lasers. To resolve the modes, we use a Fabry-Pérot filter with a bandwidth (full width at half maximum) of 10 GHz that allows us to isolate each individual longitudinal laser-cavity mode. In Fig. 2 we plot the temporal evolution of the power of one of the main modes for both lasers for a time interval that corresponds to the range $\sim$100–200 ns of panel (a) of Fig. 1. When one of the series is shifted by τ a well-synchronized dynamics can be observed.

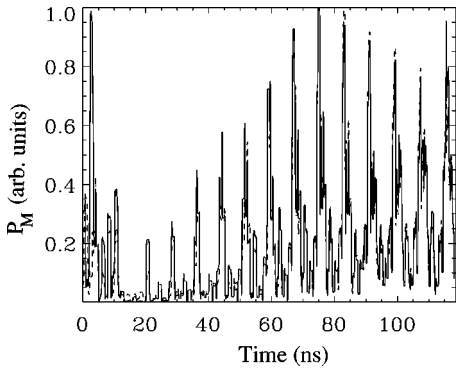

FIG. 2. Synchronization of the output power in the most intense laser-cavity mode for both lasers. One of the outputs (showed as the dashed line) is delayed by the external cavity trip time τ.

To characterize quantitatively the degree of synchronization between the different longitudinal modes of the two lasers, we compute the cross correlation function between the same longitudinal mode of the two lasers, defined as

$$S_i(\Delta t) = \frac{\langle \delta P_1^i(t)\, \delta P_2^i(t-\Delta t)\rangle}{\sqrt{\langle [\delta P_1^i(t)]^2\rangle \langle [\delta P_2^i(t)]^2\rangle}},$$

where $P_1^i(t)$ and $P_2^i(t)$ represent the output power of the ith longitudinal mode of each laser. Figure 3 shows the cross correlation functions between the total power, the power of one of the main modes [located at ~ -200 GHz in Fig. 1(b)], and the power of one side mode [in this case the one located at ~ -600 GHz in Fig. 1(b)]. In all cases we observe maxima of the cross correlation function at $\pm\tau$. In addition, we also observe correlation, although smaller, at $\pm 3\tau$, $\pm 5\tau$, etc. On the other hand, when computing the cross correlation function between *different* longitudinal laser-cavity modes, we observe almost no correlation, as can be seen in Fig. 3 (d) for the mode located at ~ -200 GHz in one laser and the one located at ~ -70 GHz in the other laser. This fact indicates that the synchronization takes place only between the same longitudinal modes of the two lasers while the correlation between different longitudinal modes is rather weak. The fact that the same longitudinal mode of the different

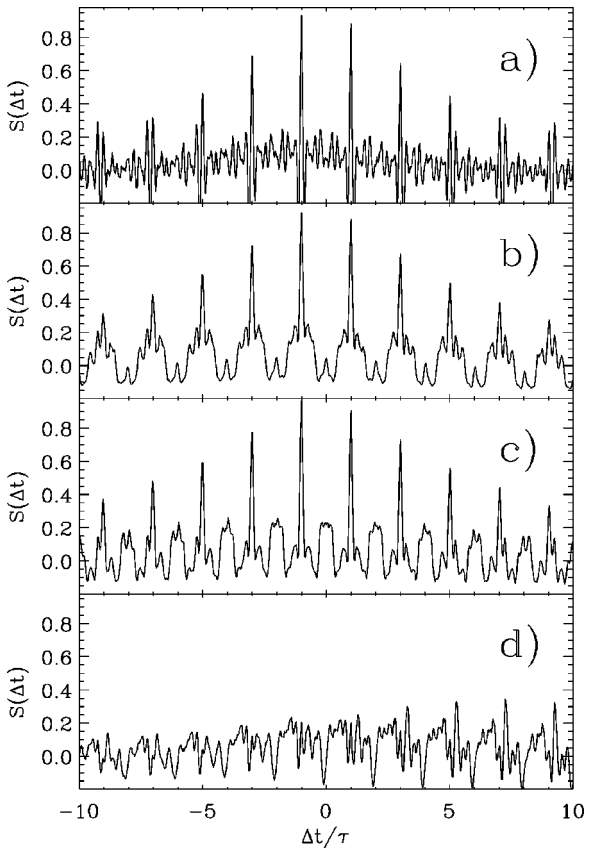

FIG. 3. Cross correlation function of the output powers of the Fabry-Pérot laser twins in (a) the total output, (b) the most intense laser-cavity mode, and (c) one of the weak side modes. (d) shows the cross correlation between different laser-cavity modes with no significant synchronization present.

lasers synchronizes was also observed in a system of two unidirectionally coupled semiconductor lasers [5].

As in the experiments and previous numerical simulations [4,8] we also observe synchronization at the sub nanosecond time scale. However, the quality of the synchronization depends on the bandwidth of the detector. In Fig. 4 we plot the correlation coefficient, or the value of the cross correlation

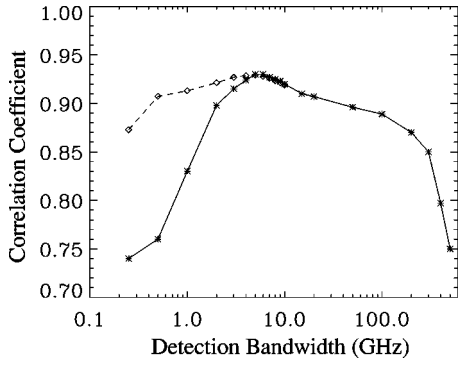

FIG. 4. Correlation coefficient as a function of the detector bandwidth. The full curve and star symbols correspond to the total output power, while the dashed line and diamond symbols, which last until 10 GHz, show the result for a single, filtered laser-cavity mode.

function calculated at a time τ, vs the bandwidth of the detector for both the main mode (dashed line) and the total intensity (solid line). The synchronization is better for the individual longitudinal modes than for the total intensity and it extends almost over the whole range of detection without losing its quality. The partial loss of synchronization in the slower-detector regime is due to the fact that the actual wave forms emitted by the lasers consist of trains of rather short pulses that are blurred when the detector response time is longer than the typical pulse duration. On the other hand, the synchronization gets worse for very fast detectors as well. This is because of the lack of synchronization between *different* laser-cavity modes and by interference effects between them. As can be noted in the figure, the detection bandwidth for the isolated longitudinal mode is restricted to frequencies up to 10 GHz because of the previous optical filtering process. In any case, it is important to remark that a high degree of synchronization is obtained for a wide detection bandwidth.

Finally, we considered a similar situation to that we have already discussed but where the lasers are now two DFB lasers. They are placed at the same distance and pumped close to threshold. The observed behavior of the output power is qualitatively similar to the one shown in Fig. 1(a). However, we observe in the optical spectra that the lasers operate mainly in one longitudinal mode and only one side mode carries a small fraction of power. As in the FP case, the spectra of both lasers are very similar to each other, indicating a high degree of synchronization. After filtering the longitudinal modes we again compute the cross correlation function. In Fig. 5 we plot this function for the two modes and for the total power. As expected, there are only small differences between the cross correlation of the total power and that of the main longitudinal mode. But it can also be seen that the side mode synchronizes to its counterpart at the same time shift $\pm\tau$, $\pm 3\tau$, etc. as do the total power and the main mode power. This again indicates that the synchronization takes place at the same mode of the different lasers.

The important difference from the FP system case is that with the DFB lasers we can identify the laser mode that is responsible for the LFF behavior. Moreover, we can directly check if the other mode, the suppressed one, plays any role in the destabilization process. In Fig. 6 we plot, for comparison, the time-dependent modal powers during two consecutive dropouts. It is important to point out that for the time traces we have a time resolution of ~ 0.1 ps. It can be clearly seen that the side mode typically exhibits measurable power only after a power dropout of the main mode develops. After the main mode recovers, the side-mode power steadily decreases until the next dropout, increasing the side-mode suppression ratio to several orders of magnitude. That is a strong indication that the side mode is actually not important for the LFF behavior and does not play any role in triggering the power dropouts. By the same token, it is also a strong indication that the single-mode models actually do capture the essential physics of the phenomenon.

In conclusion we have carried out a study of the dynamics of two distant, mutually coupled semiconductor lasers. To describe the lasers we have used a laser simulator with full

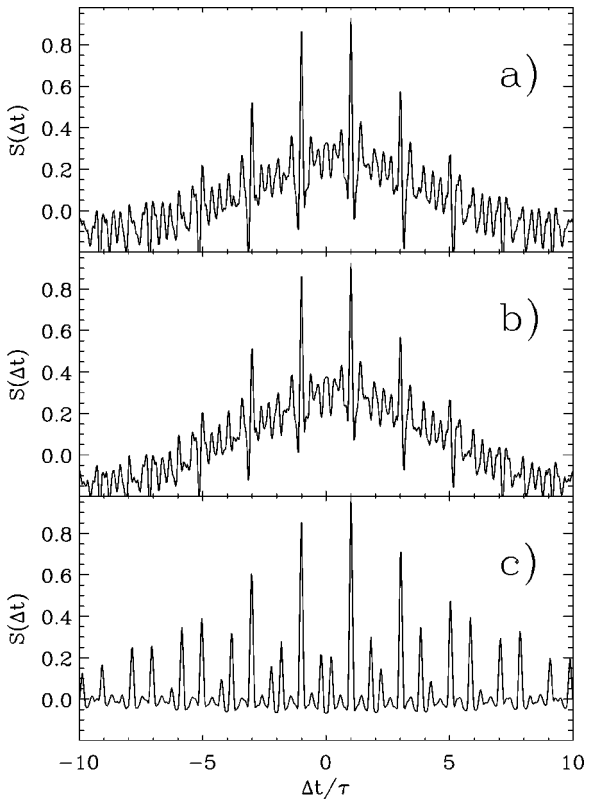

FIG. 5. Cross correlation function of the output powers of the two coupled DFB lasers. (a) and (b) show the total output power and the main mode correlations, respectively. (c) shows the cross correlation functions between the side modes of the two lasers.

spatial and temporal resolution that captures correctly the dynamics of both Fabry-Pérot and DFB lasers and includes a realistic model for the active medium. We have observed synchronization between the two output powers when one of the series is shifted with respect to the other by a time τ corresponding to the external cavity length. By filtering individual laser-cavity modes we have observed that this synchronization takes place between the same individual longitudinal modes of the two lasers. On the other hand, the degree of synchronization between *different* laser-cavity modes turns out to be much smaller. As a consequence, the quality of the synchronization is better for the individual longitudinal modes than for the total power. We have also studied coupled DFB lasers to compare a multimode regime with an essentially single-mode situation. Our findings indicate that the dynamics responsible for the LFF behavior and the output power synchronization takes place within a single laser-cavity mode. Moreover, we have also observed that the suppressed mode does not play any role in triggering the LFF.

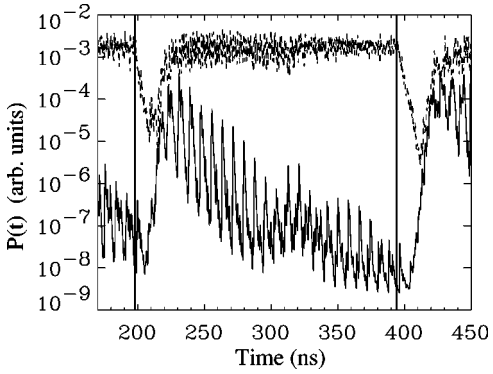

FIG. 6. Output power of the dominant mode (upper curve) and of the side mode (lower curve) of one of the DFB lasers.

This work was funded by Spanish MCyT under Projects No. TIC99-0645-C05-02 and No. BFM2000-1108, by DGES under Project No. PB97-0141-C02-01, and also by AFOSR Grant No. F4962-00-1-0002 and AFOSR DURIP Grant No. F4962-00-1-0190. M.K. was partly supported by the GASR Grant No. VEGA 2/7174/20.

[1] S.H. Strogatz and I. Stewart, Sci. Am. **269**, 68 (1993).
[2] U. Ernst, K. Pawelzik, and T. Geisel, Phys. Rev. Lett. **74**, 1570 (1995).
[3] R. Roy and K.S. Thornburg, Jr., Phys. Rev. Lett. **72**, 2009 (1994); T. Sugawara, M. Tachikawa, T. Tsukamoto, and T. Shimizu, *ibid.* **72**, 3502 (1994); K. Otsuka, R. Kawai, S.L. Hwong, J.Y. Ko, and J.L. Chern, *ibid.* **84**, 3049 (2000).
[4] T. Heil, I. Fischer, W. Elssser, J. Mulet, and C.R. Mirasso, Phys. Rev. Lett. **86**, 795 (2001).
[5] J.K. White and J.V. Moloney, Phys. Rev. A **59**, 2422 (1999).
[6] G.D. VanWiggeren and R. Roy, Science **279**, 1198 (1998); C.R. Mirasso, P. Colet, and P. Garcia-Fernandez, IEEE Photonics Technol. Lett. **8**, 299 (1996); J.P. Goedgebuer, L. Larger, and H. Porte, Phys. Rev. Lett. **80**, 2249 (1998).
[7] I. Fischer, Y. Liu, and P. Davis, Phys. Rev. A **62**, 011801(R) (2000).
[8] J. Mulet, C. Mirraso, T. Heil, and I. Fisher, Proc. SPIE **4283**, 139 (2001).
[9] G. Vaschenko, M. Guidici, J.J. Rocca, C.S. Menoni, J.R. Tredicce, and S. Balle, Phys. Rev. Lett. **81**, 5536 (1998).
[10] E.A. Viktorov and P. Mandel, Phys. Rev. Lett. **85**, 3157 (2000); J.K. White, Ph.D. dissertation, The University of Arizona, 1999.
[11] M. Kolesik and J.V. Moloney, IEEE J. Quantum Electron. **37**, 934 (2001).
[12] A. Hohl, A. Gavrielides, T. Erneux, and V. Kovanis, Phys. Rev. Lett. **78**, 4745 (1997); Phys. Rev. A **59**, 3941 (1999).
[13] G.H.M. van Tartwijk and D. Lenstra, Quantum Semiclassic. Opt. **7**, 87 (1995).